^{1}H NMR Structural Characterization of the Cytochrome *c* Modifications in a Micellar Environment

S. Chevance,[‡] E. Le Rumeur,[§] J. D. de Certaines,[§] G. Simonneaux,[‡] and A. Bondon*,[‡]

Laboratoire de Chimie Organométallique et Biologique, UMR CNRS 6509, Institut de Chimie, Université de Rennes 1, Campus de Beaulieu, 35042 Rennes Cedex, France, and Laboratoire de Résonance Magnétique en Biologie et Médicine, UPRES EA 2230, Université de Rennes 1, Campus de Villejean, 35043 Rennes Cedex, France

Received June 17, 2003; Revised Manuscript Received September 25, 2003

ABSTRACT: The interaction of cytochrome *c* with micelles of sodium dodecyl sulfate was studied by proton NMR spectroscopy. The protein/micelles ratio was found to be crucial in controlling the extent of the conformational changes in the heme crevice. Over a range of ratios between 1:30 and 1:60, the NMR spectra of the ferric form display no paramagnetic signals due to a moderately fast exchange between intermediate species on the NMR time scale. This is consistent with an interconversion of bis-histidine derivatives (His18−Fe−His26 and His18−Fe−His33). Further addition of micelles induces a high-spin species that is proposed to involve pentacoordinated iron. The resulting free binding site, also encountered in the ferrous form, is used to complex exogenous ligands such as cyanide or carbon monoxide. Attribution of the heme methyls was performed by means of exchange spectroscopy through ligand exchange or electron transfer. The heme methyl shift pattern of the micellar cyanocytochrome in the ferric low spin form is different from the pattern of both the native and the cyanide cytochrome *c* adduct, in the absence of micelles, reflecting a complete change of the heme electronic structure. Analysis of the electron self-exchange reaction between the two redox states of the micellar cyanocytochrome *c* yields a rate constant of 2.4×10^4 M^{-1} s^{-1} at 298 K, which is surprisingly close to the value observed in the native protein.

Cytochrome *c* (cyt *c*) is a hemeprotein with 104 amino acids, and was one of the first proteins to be studied by NMR spectroscopy (*1*−*3*). Histidine 18 and methionine 80 are the two axial ligands in the native form. However, several different forms have also been reported depending on the temperature, ionic strength, and pH (*4*−*6*). Several groups (*7*−*13*) have carried out full proton assignment and solution structure determination of the native protein in the two redox states. Since the first evidence of interactions between cyt *c* and sodium dodecyl sulfate (SDS) (*14*) or lipids (*15*−*17*), several studies have been performed to describe the observed structural changes of cyt *c* due to interactions with lipids (*6*, *18*−*24*). Interest in the interaction between membrane and cyt *c* was reinforced by recent evidence of an altered structure in two functions. The first concerns the electron-transfer reaction between cyt *c* and cyt *c* oxidase, one of its redox partners. Under physiological conditions, a small fraction of cyt *c* is bound to the inner mitochondrial membrane (*25*) and the associated structural changes could be responsible for modulation of the electron-transfer activity (*26*). The second function corresponds to the activation of caspases by cyt *c* during the early stages of apoptosis, while structural changes have also been described during the interaction with Apaf-1 (*27*).

In this context, we need more information on cyt *c* structural changes induced by a lipidic environment to gain a better understanding of these mechanisms. To this purpose, authors have prepared several model systems and used various techniques, the results being reviewed by T. Pinheiro (*28*). In summary, cyt *c* is able to interact with negatively charged phospholipids in a first electrostatic step followed by hydrophobic interactions with the lipid acyl chains, but the mechanism remains unclear depending on both the model system and the experimental techniques. Regarding the extent of the structural changes of the cyt *c* interacting with the phospholipids, several lines of evidence rule out a complete unfolding of the protein. While it is generally assumed that part of the solution structure is maintained, the overall dynamics of the protein and heme coordination can be greatly perturbed. The dynamic behavior has been elucidated by amide proton-deuteron exchange kinetic measurements using solution and solid-state NMR (*29*, *30*). The interaction of cyt *c* with a lipidic environment is also characterized by the disappearance of the charge-transfer band at 695 nm associated with the breaking of the S_{met80}−iron bond. However, the exact nature of the new axial ligands is not fully resolved and even the spin state of the iron seems to depend on the nature of the lipid mixture. Because NMR spectroscopy of paramagnetic hemeproteins is a powerful tool for studying the heme coordination and the spin state of the metal (*31*−*33*), NMR studies of cyt *c* in lipidic environments appear very promising.

On the basis of our previous studies on large hemeprotein complexes (*34*−*36*), we analyze here the modifications of cyt *c* in a micellar environment to mimic the behavior of cyt *c* binding to membrane. Although several studies using

* Corresponding author. Phone: 33−2−23−23−65−61. Fax: 33−2−23−23−56−37. E-mail: Arnaud.Bondon@univ-rennes1.fr.
[‡] UMR CNRS 6509.
[§] UPRES EA 2230.

10.1021/bi035044+ CCC: $25.00
Published on Web 11/25/2003

various techniques have been performed on the interaction between cyt *c* and micelles, no ^{1}H NMR data are so far been reported on such systems. The present data lead us to describe the spin-state variations of cyt *c* as a function of the protein/micelles ratio. At high molar ratio of sodium dodecyl sulfate (SDS), a low-spin to high-spin transition was detected through the characteristic heme methyl resonances around 60−80 ppm. Similar NMR results with micelles were obtained with lysophosphatidylserine, which is more closely related to natural anionic lipids. Using the free binding site of the pentacoordinated micelles-bound cyt *c*, it is possible to achieve complexation of several exogeneous ligands in both ferric and ferrous states at neutral pH, thus allowing further characterization of the heme environment of the micelles-bound cyt *c*. Of special interest is the binding of cyanide to the cyt *c*/micelles complex, which occurs in both the oxidized and the reduced states. Surprisingly, the self-exchange electron transfer reaction under such conditions occurs with a partially reduced sample. This has proved useful for proton assignment based on EXSY spectra. We estimated the self-exchange electron-transfer rate constant by means of saturation transfer experiments, obtaining a value that is very similar to the native cyt *c* without micelles.

EXPERIMENTAL PROCEDURES

Chemicals. SDS and type-IV cyt *c* from horse heart were purchased from Sigma Chemical Co. Deuterated SDS-d_{25} was purchased from Eurisotop (Saint Aubin, France). Lysophosphatidylserine was obtained from Avanti Polar Lipids (Alabaster, AL). Prior to use, cyt *c* was converted to the fully oxidized form by addition of an excess of ferricyanide $K_3Fe(CN)_6$ and then purified on a Sephadex G-10 column. Eluent containing the purified protein was concentrated by ultrafiltration using an Amicon YM-10 membrane. Ferrous cyt *c* was obtained under an argon atmosphere by reduction with a previously degassed solution of sodium dithionite. Protein concentrations were measured spectrophotometrically using molar absorption coefficients of $\epsilon_{\text{ferricyt}c} = 106\ \text{mM}^{-1}\ \text{cm}^{-1}$ at 410 nm or $\epsilon_{\text{ferrocyt}c} = 29.5\ \text{mM}^{-1}\ \text{cm}^{-1}$ at 550 nm at pH 7.0. All micellar or ligand solutions added to reduced cyt *c* were flushed with argon (or CO) to prevent protein oxidation.

Spectrophotometric Titration by Micelles. All the absorption spectra were recorded in a cuvette of 1-cm path length at room temperature on an UVIKONXL spectrophotometer (Bio-Tek Instruments). Microliter aliquots of 1 M SDS solution in 10 mM Tris-HCl buffer pH 7.0 were sequentially added to a fully oxidized or reduced 10 μM solution of cyt *c* in the same buffer until no further modification of the spectra was detected. The highest SDS concentrations used were comprised between 10 and 12 mM.

NMR Spectroscopy. ^{1}H NMR spectra were recorded on a Bruker AVANCE DMX 500 at 500.13 MHz with a 5-mm reverse dual ^{1}H-^{13}C probe. ^{1}H NMR (1D or 2D) spectra of the low-spin ferric and diamagnetic forms were recorded using a sweep width of 30 and 8 kHz, respectively. A larger window (100 kHz) was used for detection of the high-spin forms of ferricyt *c* and ferrocyt *c* induced by SDS micelles. The spectra were acquired with a 90° reading pulse using the PASE method (*34*) with a shorter acquisition time (20 ms).

We obtained 2D NMR NOESY spectra of the high-spin ferric form of micellar cyt *c* and EXSY spectra through ligand exchange between the micellar high-spin form and the micellar low-spin cyanoferricyt *c*. The analyses were performed using nondeuterated SDS by means of the PASE method as previously reported (*34*, *36*). The spectra were acquired in the TPPI mode using short presaturation of the residual water followed by a broadband decoupling time of 100 ms. A mixing time of 5 ms was used. EXSY spectra between the two redox states of the micellar cyano adduct of cyt *c* were acquired by suppressing the SDS signals using presaturation with a frequency list comprising the main SDS signals.

2D NMR spectra of the diamagnetic forms of micellar cyt *c* were mostly obtained with deuterated SDS-d_{25} and recorded with mixing times of 250 ms. We also carried out NMR transfer saturation experiments to determine the electron-transfer rates with deuterated micelles to obtain values that are more accurate.

NMR Titration Experiments. We performed titrations of 1 mM ferri- or ferro-cyt *c* solution in 10 mM Tris-HCl pD 7.0 by adding aliquots of SDS stock solution (0.5 or 1 M) prepared in the same buffer. For titration experiments in the presence of exogenous ligands, cyanide or CO was first added to the protein solution. The range of SDS concentrations used was 0−130 mM. The one-dimensional ^{1}H NMR spectra were recorded at 298 K for each SDS addition, after 15 min for equilibration.

Structural and Functional Experiments. We prepared a 1 mM solution of micelles-bound cyt *c* (with a protein/detergent molar ratio of 1:110) with or without exogenous ligands, and then transferred it into a previously degassed NMR tube. For mixed samples of ferric and ferrous cyt *c*, we prepared a fully oxidized 1 mM solution of cyt *c* and added a degassed dithionite solution (100 mg/mL) μL by μL until the desired redox level was attained. Because the micellar cyt *c* is very sensitive to the oxidation with traces of oxygen, the redox level was determined, after addition of micelles, by integration of heme methyl signals and comparison with the fully oxidized sample taken as a reference.

Determination of Self-Exchange Electron-Transfer Rate. NMR saturation transfer experiments were performed on partially reduced cyanocyt *c* solution (mixture of Fe^{III}-CN/Fe^{II}-CN) in deuterated SDS micelles (cyt *c*/dSDS molar ratio of 1:100) at pD 7.5. The magnetization transfer between the two redox species was induced by irradiation of the cyanoferricyt *c* heme methyl using different irradiation times from 10 to several hundred milliseconds. Difference spectroscopy was used and the areas of the corresponding signals in the cyanoferrocyt *c* form were measured by integration. The electron transfer can be written as a chemical exchange reaction as follows:

$$\text{cyt } c\ \text{Fe}^{\text{III}}-\text{CN} + \text{cyt* } c\ \text{Fe}^{\text{II}}-\text{CN} \underset{k_{-1}}{\overset{k_1}{\rightleftharpoons}} \text{cyt } c\ \text{Fe}^{\text{II}}-\text{CN} + \text{cyt* } c\ \text{Fe}^{\text{III}}-\text{CN}$$

The extent of the magnetization transfer, from the ferric form to the ferrous form, is related to the longitudinal relaxation rate of the ferrous signal, T_1^{Red} (without any ferric form present), and the electron-transfer rate, k (*37*). The plot of the magnetization transfer build-up, M_t, versus

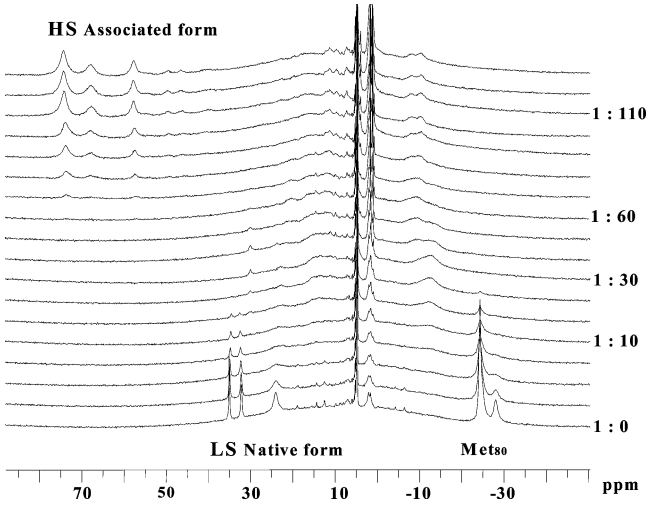

FIGURE 1: ^{1}H NMR PASE spectra of a 1 mM cyt *c* Fe^{III} solution in 10 mM Tris-HCl D_2O buffer, pD 7.0, at 298 K, after successive addition of a 1 M SDS solution prepared in the same buffer. Protein/micelles molar ratios are indicated.

the irradiation time (t) of a ferric signal was analyzed as previously reported for the intermolecular electron-transfer rate of the binary complex of cyt P450cam and putidaredoxin (*35*). The curve was fitted according to the following relation:

$$\frac{M_0 - M_t}{M_0 - M_\infty} = (1 - e^{(t/T_1^{App})})$$

where M_0 and M_∞ denote the magnetization with or without infinite saturation, respectively.

T_1^{App} represents the apparent relaxation time of the ferrous methyl protons in the presence of electron self-exchange. The self-exchange electron rate constant is not only related to T_1^{App} but also to the relaxation time of the reduced form and the concentration of oxidized cyt *c* as follows:

$$k_1 = \left(\frac{1}{T_1^{App}} - \frac{1}{T_1^{Red}}\right)\cdot\frac{1}{[Ox]}$$

The heme methyl relaxation time of the pure reduced form is not accessible because the methyl proton resonances are under the crowded aliphatic region. However, when the electron-transfer rate is fast enough compared to the relaxation rate (*35*), this rate does not contribute significantly to the calculated value of k_1.

RESULTS

Titrations of Cytochrome c by Micelles. The titration of ferric cyt *c* against increasing amounts of SDS at pH 7.0 is illustrated in Figure 1. The spectra were acquired with the PASE sequence using the saturation of the entire diamagnetic region. This method improves the quality of the paramagnetic signal detection owing to a better baseline and removal of the 0−10 ppm peaks (*34*). This latter feature is particularly useful in the present study, which involved adding large amounts of protonated SDS. Under these conditions, the signals close to the diamagnetic region were also partially suppressed. The first spectrum (Figure 1, bottom) is characteristic of the native form of cyt *c*, with two heme methyl signals at 33 and 35 ppm and protons of the bound methionine around −25 ppm. Progressive addition of SDS led to a decrease of these signals, which finally disappeared at a cyt *c*/SDS molar ratio of 1:30. This observation is in good agreement with the previously reported rupture of the methionine−iron bond detected through the disappearance of the 695 nm charge-transfer band (*21*). With further increase in SDS concentration, heme methyl peaks, corresponding to a high-spin ferricyt *c* species, appeared in the 50−80 ppm region for a cyt *c*/SDS molar ratio of 1:60. The maximum intensity of these heme signals was obtained at a cyt *c*/SDS molar ratio of 1:110.

Surprisingly, no paramagnetic shifted signals were resolved in the spectra acquired in the range from 288 to 313 K, between the two well-defined native and high-spin forms. This absence of detectable signals is probably due to a moderately fast (or quasi slow) exchange, on the NMR time scale, between different forms of cyt *c*. Furthermore, during the titration, there was very little broadening of either the decreasing low-spin signals or the increasing high-spin resonances. This indicates that neither the high-spin nor the low-spin forms were involved in this chemical exchange. Thus, following the rupture of the methionine iron bond, rapid equilibrium should be attained with other forms containing iron coordinated by different residues. Lys 73 or Lys 79 have been shown to be the two most likely candidates for the sixth ligand of the alkaline forms (*38*, *39*). However, amino groups are protonated at pH 7.0 and binding of these amino acids is precluded. Two other heme sixth ligands, His 26 and His 33, have already been proposed as intermediate during the folding−unfolding of cyt *c* (*40*−*42*). Furthermore, these histidines are also thought to be involved in the hexacoordinated low-spin cyt *c* form observed during the interaction with micelles at low protein/SDS molar ratio (*6*, *21*, *24*). In this way, the observed signal broadening at intermediate protein/micelles ratio is in good agreement with an exchange of these two histidines as sixth ligand. Support for this interpretation comes from the titration of reduced cyt *c* performed in the presence of exogenous ligand such as cyanide or carbon monoxide (see below).

Since pH is an important factor influencing the line width of the high-spin heme methyl resonances, the signals were better resolved at pH 6.0, as shown in Figure 2A. Under such conditions, the spectra are well resolved and any meso-resonances in the downfield region are ruled out. The resonances of the meso protons are characteristic of high-spin species. Some studies have clearly demonstrated that hexacoordinated species (His−Fe−H_2O) contain heme meso protons around 40 ppm, whereas the pentacoordinated species (without any water molecule) display meso resonances around −20 ppm (*43*). These meso protons could account for the broad resonances observed at neutral pH around −20 ppm. However, these peaks were not detectable in slightly acidic conditions, in agreement with the behavior already described for a pentacoordinated cyt *c*′ from *Chromatium vinosum* (*44*).

We performed progressive addition of another anionic surfactant (lysophosphatidylserine or lysoPS), which is more closely related to the natural phospholipids. Similar spectra were observed with the same molar ratio dependence, indicating identical modifications of the ferricyt *c* active site. Figure 2B shows a representative spectrum of the high-spin cyt *c*-lysoPS at pH 6.0. Taken together, these results show that cyt *c*/SDS molar ratio plays a crucial role in the induction

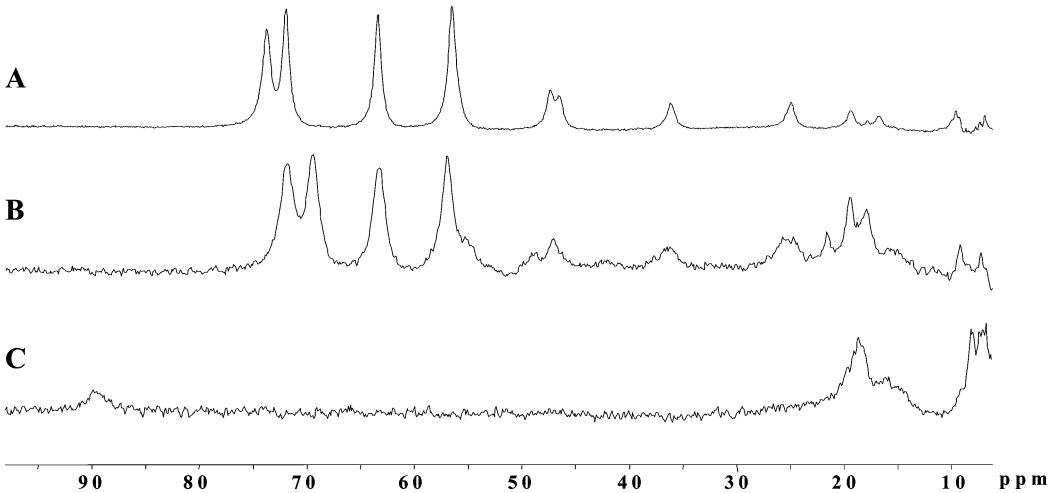

FIGURE 2: ^{1}H NMR PASE spectra of different HS cyt *c* non-native forms acquired at 298 K, pH 6.0. (A) SDS-bound ferricyt *c* in D_2O; (B) LysoPS-bound ferricyt *c* in D_2O; (C) SDS-bound ferrocyt *c* in H_2O.

of protein structural changes. At low protein/micelles ratios (up to 1:30), detergents are able to interact with cyt *c* and induce structural changes such as breaking of the Fe^{III}−SMet80 axial bond. However, further increase of this ratio (from 1:30 to 1:60), far above the critical micellar concentration (cmc), does not lead to the formation of high-spin ferricyt *c*, when the protein is in the high concentration range (mM) required for the NMR experiments. Finally, pure high-spin ferricyt *c* was only observed at a ratio as high as 1:110.

Titration of SDS micelles against reduced cyt *c* yielded a decrease of the native form signals, which totally disappear at a protein/micelles ratio of 1:40. Further increase of the ratio leads to the appearance of broad resonances in the 10−20 ppm region (Figure 2C). This spectrum corresponds to the formation of a pentacoordinated high-spin species, and is closely similar to the spectrum of the deoxy myoglobin (*31*, *45*, *46*) and the reduced cyt *c*′ from *Rhodopseudomonas palustris* (*47*). Of special interest is the presence of an exchangeable broad peak at very low field, close to 90 ppm (Figure 2). A similar signal was also observed in deoxyMb and reduced cyt *c*′, which has previously been assigned to the proximal His $N_\delta H$ (*46*, *47*). We may thus assign the peak at 90 ppm to His18 $N_\delta H$, suggesting that this histidine, representing the native ligand of the heme, remains ligated to the iron in the ferrous high-spin form. The disruption of this histidine has previously been proposed for micellar cyt *c* (*48*). However, the broad line width of the heme methyl resonances prevents any assignment of these paramagnetic signals, in contrast with the relatively sharp peaks observed at pH 6.0 with the ferric high-spin form of the micellar cyt *c*. To illustrate this, we present a 2D NOESY spectrum of the ferric form in Figure 3. Despite the use of unlabeled SDS micelles, a well-defined 2D spectrum can be obtained by use of the PASE method, which allows the detection of several cross-peaks useful for the assignment of paramagnetically shifted resonances. For example, heme methyls belonging to pyrrole III and IV were easily identified at 73.8 and 64.7 ppm through cross-peaks with propioniate side-chain protons. Further assignments were performed with the help of EXSY spectra (see below).

Complexation of Exogenous Ligands of Micellar cyt c in Ferric and Ferrous States. The titration experiments described above point out the crucial role of the protein/detergent molar ratio in the detection of high spin state NMR signals. Met80 exchange is easily achieved on the native ferric cyt *c* by addition of cyanide, azide, pyridine, imidazole, or phosphine, which give stable complexes (*49*−*53*).

In the reduced form, the iron−methionine bond has been shown to be very strong, and any binding of exogenous ligand would require disruption of this bond. This can be carried out through alkylation of the distal methionine or by increasing the pH above the alkaline transition. One exception is the binding of the trimethylphosphine ligand. When this bulky ligand is complexed to ferric cyt *c*, the iron can be reduced without causing its departure. This has been previously associated with the large steric influence of this ligand, which prevents the methionine from returning to the iron (*54*). However, the more usual way of forming new complexes is to alkylate the Met80 sulfur atom creating a free binding site. Such an approach has been used by carboxymethylation of the methionine (DMC-cyt *c*) (*55*). Also relevant here is the carbon monoxide binding on reduced carbodi-imide-modified cyt *c*. A stable complex is observed with a spectrum (*56*) similar to that obtained for cyt *c* $Fe^{II}CO$ at very high pH (*57*). In the present study, an important point in the use of micelles is the access to a free binding site for exogenous ligands in both redox states. Figure 4 shows the NMR titration of SDS against the cyanide ferric cyt *c* derivative. Without micelles the spectra of ferricyano cyt *c* is similar to those previously reported (*58*−*60*). During the addition of micelles, the heme methyl signals of this form rapidly weaken and cancel out around a ratio of 1:25, whereas the peaks of the micellar form show a concomitant rise. The line width of these heme methyls attains 500 Hz for a molar ratio of 1:20 and falls to 80 Hz for a molar ratio of 1:100. The broadening of the signals suggests a relatively rapid equilibrium between the two forms, the native cyano- and the micellar cyanoferri-cyt *c*. However, at a low protein/SDS ratio around 1:20, when both sets of signals were present, we failed to observe saturation transfer between the native and the micellar forms. Furthermore, increasing the temperature to 313 K induced partial precipitation of the sample. However, both the cyanide adducts of cyt *c* in the native and the micellar (at a ratio 1:100) forms were stable up to 323 K. These observations suggest that some intermediate(s) exist with lower thermal

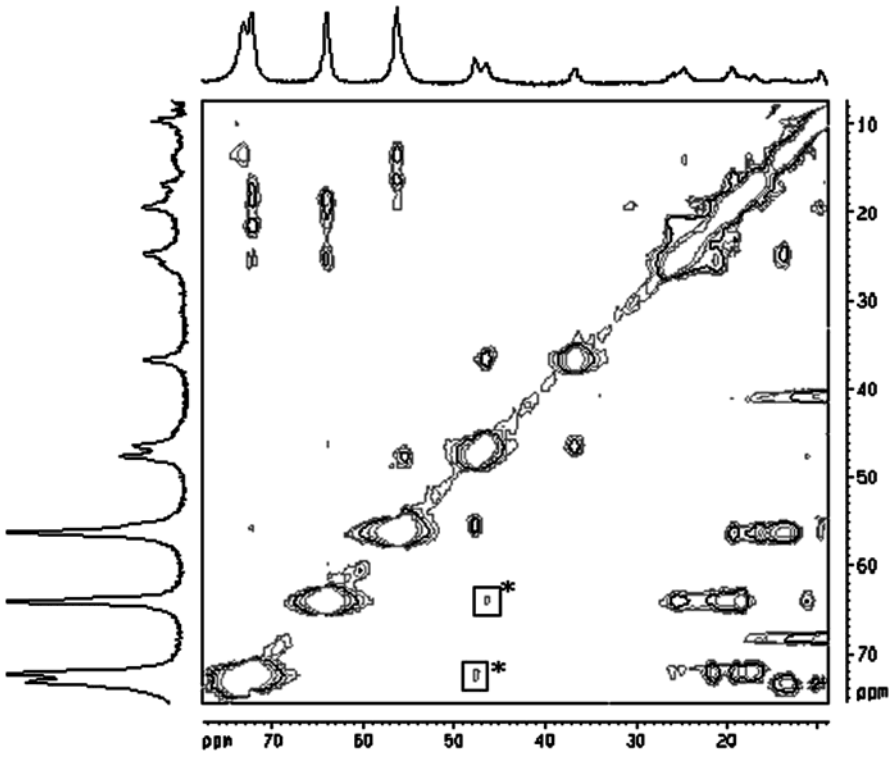

FIGURE 3: 2D PASE NOESY (*34*) spectrum of cyt *c*/SDS (1:110) pD 6.0, at 313 K. The spectrum was acquired in TPPI mode using short presaturation of the residual water followed by a broadband decoupling of 100 ms. A mixing time of 5 ms was used. Asterisks denote methyl-propionate cross-peaks.

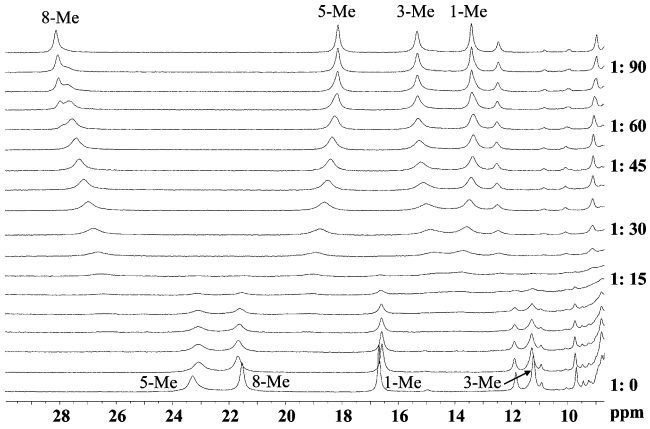

FIGURE 4: ^{1}H NMR spectra of a 1 mM cyt *c* Fe^{III}-CN solution in 10 mM Tris-HCl D_2O buffer, pD 7.0, at 298 K, after successive addition of 1 M SDS aliquots. Protein:micelles molar ratios are indicated. The heme methyls resonances are labeled for both species, without micelles from refs *58*−*60*.

stability during the conversion of the cyanoferricyt *c* into the micellar form.

We observed a fine-tuning of the chemical shift of the 8-heme methyl signal (see Table 2, see below) from 27.7 to 28.0 ppm when the cyt *c*/SDS ratio varied from 1:60 to 1:100. Although such a local heterogeneity in the heme vicinity of ferric cyt *c* has already been reported for the native form, this was at the expense of the 3-heme methyl signal (*61*, *62*). The origin of these two exchanging conformations has been linked to the motion of the His33 (*63*). In the present study, we do not identify the residue responsible for these variations, but this observation further suggests that fine-tuning of the heme pocket remains possible even in the micellar form of cyt *c*.

We used spectrophotometry to monitor the progressive addition of SDS micelles on native reduced cyt *c*. The spectra without cyanide are displayed in Figure 5A. As previously reported (*21*), addition of SDS induced, without intermediate, spectral changes from native low spin to high spin spectrum. In presence of sodium cyanide (Figure 5B), the bands of the native form at 415, 520, and 550 nm show a clear decrease with the concomitant appearance of maximum absorptions at 420, 525, and 555 nm with isobestic points. These values are close to those observed in the spectrum of the ferrous cyanoDMC-cyt *c* (*64*) (see Table 1). The titration was also monitored by NMR spectroscopy. This experiment was performed in the presence of 100 mM cyanide because of the weak affinity for ferrous hemeprotein. Indeed, transient complexation of cyanide has been observed with various myoglobins (*65*). However, stable adduct with DMC-cyt *c* has already been reported (*51*, *64*). As observed in Figure 6, the increase in the cyt *c*/SDS molar ratio induces (i) a weakening of the native-form signals with disappearance around 1:60 and (ii) growth of the micellar reduced cyano cyt *c* peaks, exhibiting a maximum around 1:100. Interestingly, at intermediate cyt *c*/SDS molar ratio the two sets of resonances, corresponding to the native ferrous cyt *c* and the micellar ferro cyano cyt *c*, can be observed. Also noticeable is the increase of the proton−deuteron exchange rate. The spectrum without any micelles corresponds to a freshly prepared cyt *c* solution in D_2O with remaining exchangeable protons. Upon addition of SDS, all these exchangeable proton resonances vanished in good agreement with a more open structure of the protein.

The same behavior was observed when we carried out progressive SDS addition on a ferrous cyt *c* solution under a carbon monoxide atmosphere. Both UV−visible and NMR

Table 1: Electronic Absorption Data for Various Forms of Cyt *c*

	native cyt *c* His18/Met80	native cyano cyt *c* His18/CN^-	micelle-bound cyano cyt *c* His18/CN^-	micelle-bound CO complex His18/CO	micelle-bound HS form His18
Fe^{III} Soret	410 nm, 530, 695 nm	413 nm	413 nm	no complexation	400 nm, 517, 628 nm
Fe^{II} Soret α, β	415 nm, 520, 550 nm	no complexation	420 nm, 525, 555 nm	415 nm, 530, 560 nm	420, 425 nm 480−530 nm

Table 2: ^1H Chemical Shifts (ppm) and Shift Pattern of Heme Methyls for Various Forms of Horse Heart Cyt *c* in Both Redox States at pH 7.0 and 313 K

		1-CH_3	3-CH_3	5-CH_3	8-CH_3	shift pattern
Fe^{III} native	His18/Met80[a]	6.8	33.1	9.7	35.9	8 > 3 ≫ 5 > 1
	His18/CN^-[b]	16.5	11.4	23.0	21.5	5 > 8 > 1 > 3
micellar	His18/CN^-	13.2	14.9	18.0	26.9	8 ≫ 5 > 3 > 1
	His18/−[c]	58.6	76.5	73.8	64.7	3 > 5 > 8 > 1
Fe^{II} native	His18/Met80[a]	3.52	3.85	3.61	2.18	3 > 5 > 1 > 8
micellar	His18/CN^-	3.69	3.46	3.74	3.40	5 > 1 > 3 > 8
	His18/CO	3.65	3.46	3.71	3.35	5 > 1 > 3 > 8

[a] Ref *79* and refs therein. [b] Ref *52*. [c] Experiment realized at pH 6.0 where the 3- and 5-methyl resonances are resolved.

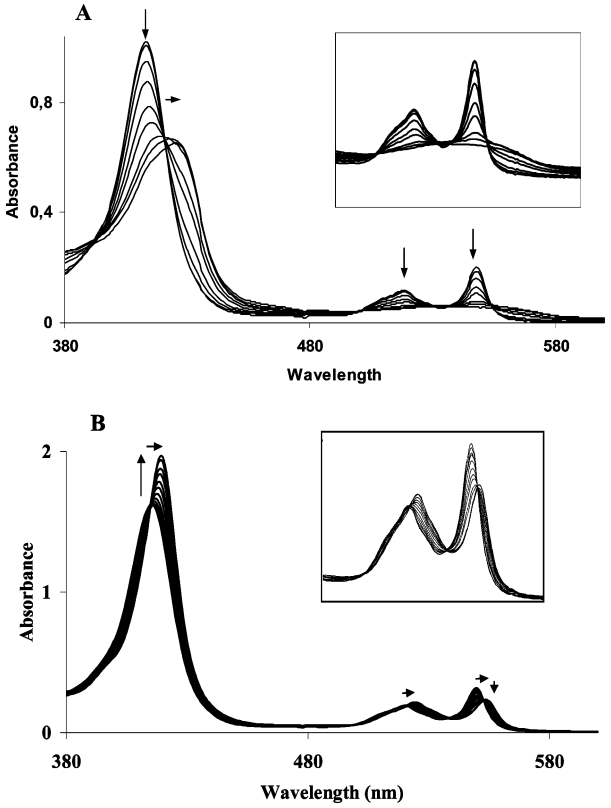

FIGURE 5: Spectrophotometric titration of reduced cyt *c* in the presence (A) or absence (B) of cyanide by progressive addition of SDS micelles.

(data not shown) are in agreement with a direct conversion of the native form to the micellar reduced cyt *c*-CO. The full decrease of the native NMR signals was observed around a molar ratio of 1:60, whereas a decrease of the line widths of the new signals was observed up to 1:100. As previously described with cyanide, both sets of resonances were present at intermediate cyt *c*/SDS molar ratio.

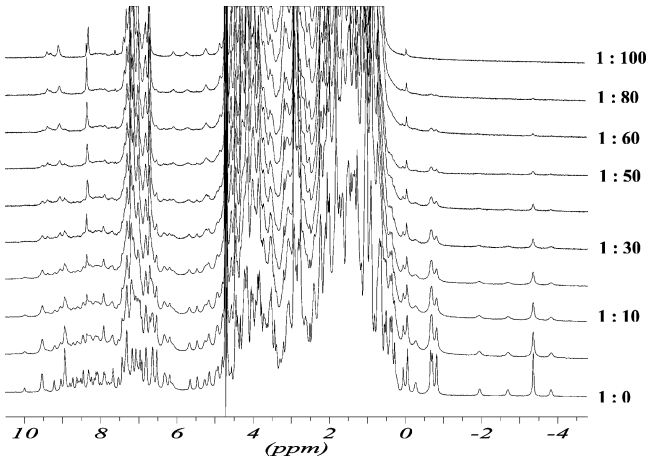

FIGURE 6: ^1H NMR spectra of a 1 mM cyt *c* Fe^{II} solution in the presence of 100 mM sodium cyanide in phosphate buffer, pD 7.0, at 298 K, after successive addition of 1 M SDS aliquots. Protein/micelles molar ratios are indicated.

Heme Proton Assignment in Both Redox States. Overall, we were able to study several derivatives of the micellar cyt *c*: HS ferric, HS ferrous, LS cyano adduct, diamagnetic cyano, and carbon monoxide ferrous adducts. Some assignments were performed through the combination of two-dimensional NOESY or EXSY spectra recorded on a mixture of ferric micellar cyt *c* partially ligated with cyanide, under ligand exchange control. Others were carried out using partially reduced micellar cyano cyt *c* under electron self-exchange control. Unfortunately, we were unable to obtain any EXSY spectra, either on native ferric cyt *c* or cyanoferricyt *c* derivative, under the same conditions (low protein/SDS molar ratio) when the corresponding micellar forms were also present. Thus, specific assignment of the heme signals requires a fuller analysis of the different spectra. For the high-spin form, the methyl signals at 73.8 and 64.7 ppm are assigned to the heme methyls belonging to the pyrroles III and IV, based on cross-peaks in the NOESY spectrum, with propionate side-chain protons (Figure 3). The EXSY spectrum of micellar cyt *c* solution partially saturated with cyanide allows us to link the paramagnetically shifted peaks of the high-spin form with the low-spin cyano form (data not shown). For example, the heme methyl signal at 73.8 ppm in the HS state is observed at 14.6 ppm in the LS state. Many studies have made use of EXSY spectra based on the electron self-exchange reaction between the two redox states of cyt *c* to correlate the ferric and the ferrous forms (*37*). In the micellar system, the ferric and ferrous forms of the cyanide derivative are able to transfer electrons at a rate compatible with EXSY experiments (Figure 7). Thus, the methyl protons resonating at 14.6 ppm in the ferric form exhibit a cross-peak at 3.56 ppm in the ferrous form. Specific assignment of this heme methyl is based on the NOESY spectrum of the diamagnetic ferrous micellar cyano cyt *c*.

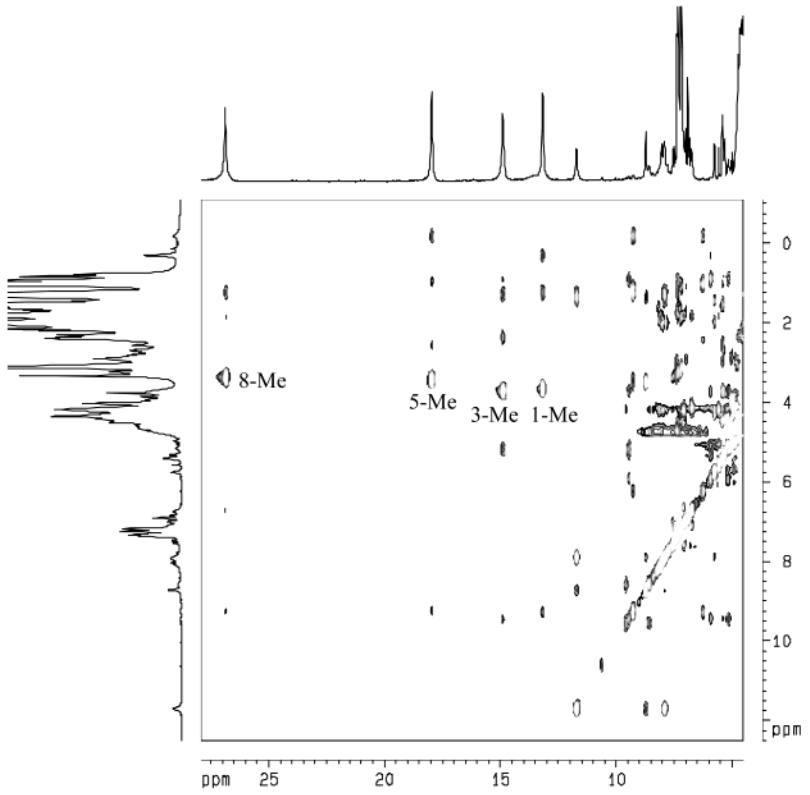

FIGURE 7: 2D EXSY spectrum of partially reduced cyt *c* Fe^{III}-CN solution in the presence of SDS at a ratio of 1/110. A mixing time of 50 ms was used. The strong cross-peak correlations between the two redox forms of the heme methyl protons through electron self-exchange are labeled.

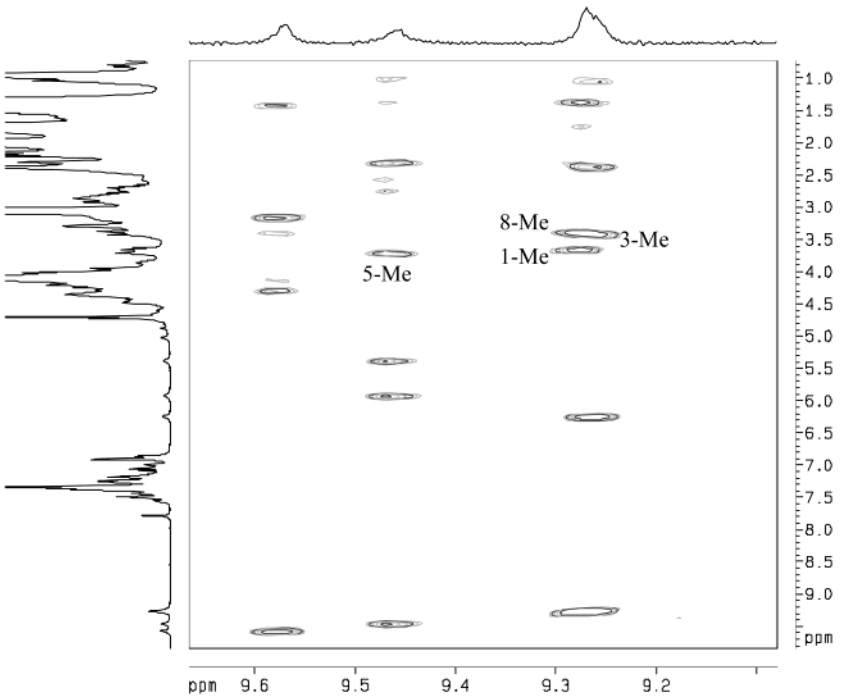

FIGURE 8: 2D NOESY spectrum of micellar Fe^{II}-CN cyt *c*: SDS (1:110) at 313 K. The spectrum was acquired in TPPI mode using several cycles of SDS signal presaturation. The residual water was suppressed by a Watergate sequence prior to acquisition. A mixing time of 250 ms was used.

Figure 8 shows a low-field part of the spectrum comprising the meso protons, which are observed at 9.57, 9.46, 9.27, and 9.25 ppm. The meso proton yielding a dipolar connectivity with only one methyl at 3.56 ppm (previously shown to belong to pyrrole III or IV) is assigned to the β-meso, while the methyl is assigned to the 5-methyl. Consequently, the cross-peak observed at 9.25 ppm/3.46 ppm is assigned to the α-meso and the 3-methyl protons. The meso proton at 9.27 ppm is located close to two heme methyls and should therefore be assigned to the δ-meso. Methyls 1- and 8- can be differentiated by means of the dipolar interaction of the 8-methyl with the 7-propionic side

chain previously observed in the HS state. Thus, through the combination of NOESY and EXSY spectra, we are able to assign several resonances in various spin states of both redox forms of cyt *c* in a micellar environment. Table 2 reports the assignment as well as the shift pattern of the heme methyls. Clearly, SDS micelles are expected to induce structural variations of the cyt *c* with large modifications of the heme electronic structure. This is particularly explicit when comparing the ferric cyano cyt *c* with and without micelles. Both species are low spin and have different heme methyls shift pattern reflecting different axial ligand geometry. Concerning the HS state of the micellar cyt *c*, the chemical shifts fall in the classical range already encountered for different hemeproteins with an axial histidine as ligand, such as metMb or ferricyt *c*′ (*31*). However, the methyl shift pattern is different between these proteins. This may be related to a different geometry of the axial histidine.

Self-Exchange Electron Transfer of Micellar Cyanocytochrome c. As pointed out above, a mixture of ferric and ferrous cyanocyt *c* bound to SDS micelles exhibits self-exchange electron transfer at a relatively high rate. Therefore, we performed some NMR magnetization transfer experiments to estimate the reaction rate. First, we tried to detect any self-exchange electron transfer between the two redox forms of a partially reduced sample of micellar cyt *c*, without an exogenous ligand. We failed to detect any magnetization transfer, indicating either the absence of electron transfer or a very fast relaxation rate of both high-spin ferric and ferrous signals which prevents the detection of saturation transfer. Cyanide yields stable complexes with micellar cyt *c*, both in the ferric and the ferrous states, so its presence is required for the detection of electron transfer. This is consistent with a low energy of reorganization between the two redox states, which is in favor of a rapid electron self-exchange. The magnetization transfer between the two redox species was induced by irradiation of a paramagnetically shifted heme methyl. Because the corresponding micellar ferrous cyt *c* heme methyls resonate under the very intense diamagnetic region of the protein−micelles complex, these signals were detected in the spectrum difference mode (data not shown). The observed signal intensity was measured for different irradiation times of the ferric resonance. According to the experimental procedure, we fitted the curve of the time-dependent saturation transfer and estimated the bimolecular rate constant as equal to 2.5×10^4 M^{-1} s^{-1} at 298 K. The ionic strength is an important parameter in the self-exchange reaction, especially with a charged protein such as cyt *c* (*54*, *66*). Hence, to compare the micellar cyt *c* with native cyt *c*, we carried out the same experiments with the native protein in the presence of 100 mM sodium sulfate. At 298 K, we estimate an electron self-exchange rate constant of 2.4×10^4 M^{-1} s^{-1}, very close to the value obtained in the presence of micelles. However, in the case of the micellar system, the observed rate constant corresponds to the true micellar self-exchange reaction. Indeed, the bonding of the cyanide ligand to the ferrous cyt *c* requires the association of the protein with micelles. This precludes the observation of an electron self-exchange reaction that involves any free protein. Preliminary results do not show any dependence of protein concentration on the rate constant, which is in favor of intermicelles reactions. Nevertheless, further work will be necessary to obtain a better description of the relations controlling electron self-exchange of cyt *c* in micelles.

DISCUSSION

The present results support the high versatility of the iron coordination induced by the interaction of cyt *c* with micelles. The influence of the cyt *c*/micelles ratio is demonstrated to be very important and dependent on the oxidation state as well as the presence or the absence of an exogenous ligand. The relatively high protein concentrations used for NMR studies require SDS concentrations far in excess of the critic micellar concentration (cmc). For SDS, the cmc at 298 K and pH 7.0 is between 4.5 mM in 10 mM phosphate buffer and 8.3 mM in nonbuffered solution (*23*). Thus, all the NMR-detected conformational changes we reported here are obtained with a micellar concentration above the cmc, in contrast with most other spectroscopies using much lower protein concentrations (micromolar). Under such conditions, it is sometimes difficult to discriminate between the protein/micelles ratio and the influence of cmc.

In the present study, each system is characterized by a set of heme methyl resonances. These signals decrease with the progressive addition of micelles and then disappear completely at a specific protein/SDS ratio. In the case of the ferric derivatives, these ratios are 1:30 and 1:25 for the native and the cyanocyt *c*, respectively. Thus, the breaking of the iron−methionine bond (already achieved in the case of the cyanide derivative) does not appear to be a key factor in triggering structural variations. The main difference associated with the presence of cyanide is the gradual increase, along with the protein/micelles ratio, of the heme methyl signals corresponding to the micellar cyanoferricyt *c*. In contrast, with the micelle-free protein, the NMR peaks of the high-spin form are only detected at a protein/micelles ratio higher than 1:60. Between 1:30 and 1:60, the absence of paramagnetic peaks is associated with exchanging species, on the NMR time scale. Evidence for the involvement of the coordination state of the iron, rather that specific interaction of micelles with the overall protein was provided by the titration of reduced cyt *c* in the presence of exogenous ligand. In such a case, direct conversion of the native form to the micellar ligand bound was observed. Yoshimura (*21*) first proposed histidine as the sixth ligand of the low-spin form of micellar cyt *c*. More recently, equilibrium was proposed between His26 and His33 (*40*) and kinetic studies by several groups investigating the cyt *c* folding (*67*−*69*) have demonstrated an exchange between these histidines as the sixth ligand of the heme iron. A similar behavior has been recently proposed in the case of the interaction of cyt *c* with lipid or micelle interactions (*6*, *24*). Our present NMR data are consistent with the existence of an exchange between two hexacoordinated low-spin species, His18−Fe−His26 and His18−Fe−His33.

With a cyt *c*/SDS ratio higher than 1:60, the chemical shifts of the heme methyls are characteristic of a high-spin heme iron. Although the signals are clearly detected at neutral pH, significant narrowing is encountered at lower pH. The good resolution obtained at pH 6 allows us to assume that there are no broad resonances around 40 ppm. Such signals have previously been assigned to the meso protons of hexacoordinated high-spin hemeproteins (*43*). The corresponding

signals of the pentacoordinated high-spin hemeprotein are localized around −20 ppm. Such broad peaks are present in the spectra at neutral pH, suggesting that the micellar cyt *c* is a pentacoordinated species. This is in good agreement with the results obtained by Raman resonance (*6*, *42*, *70*, *71*). Oellerich et al. (*6*) previously proposed a difference in the iron coordination of the non-native forms obtained through (i) the interaction with micelles (or lipid vesicles) or (ii) the addition of a denaturing agent such guanidinium chloride. Lipid-induced modifications were related to a pentacoordinated species, whereas the denaturated form was assigned to a hexacoordinated species with a water molecule as the sixth ligand (*6*).

Concerning the native ferrous form, addition of SDS micelles induces the formation of a pentacoordinated high-spin species characterized by broad resonances of the heme methyls in the 12−20 ppm region. Furthermore, a signal at 90 ppm is assigned to the His18 $N_\delta H$ by analogy with other hemeproteins (*46*, *47*). This demonstrates that the native His18 remains bound to the iron. Titrations of ferrous cyt *c* performed in the presence of CO or CN^- showed sharp NMR signals of the micellar form at a protein/micelles ratio of around 1:100. Interestingly, during the titration two sets of resonances corresponding to the native and the ligand bound species were observed in good agreement with the absence of intermediate as observed in the spectrophotometric titration. With a ratio of 1:60, we achieved a complete attenuation of the micelle-free ferrous form resonances. This value is higher than observed with the ferric derivatives, and may be related to the stronger iron methionine bond in the ferrous state. It seems that the breaking of this bond in the ferrous state is related rather to global conformational changes of the ferrous cyt *c* structure, in contrast with the ferric form. In the ferric state, exogenous ligands can displace the methionine without causing drastic structural changes as indicated by several structural studies, performed in solution, with ligands such as cyanide (*52*, *72*), imidazole (*73*), pyridine (*74*), or azide (*53*). Cyt *c* is a protein that has been extensively studied as a model of the folding process. External ligands have often been employed to mimic intermediates encountered during the folding or unfolding of cyt *c*. In the present case, we used cyanide and carbon monoxide to obtain a better characterization of the micellar form. Thus, assignment of the heme methyl resonances was performed for all the studied derivatives except the high-spin ferrous form.

Previous studies on denatured forms of cyt *c* induced at very low pH or interactions with guanidinium hydrochloride demonstrate that the high-spin transition is associated with large structural changes (*6*, *24*, *75*, *76*). By contrast, non-native conformations of cyt *c* in the presence of micelles was proposed to maintain the helical secondary structure. This is based on various studies using fluorescence, circular dichroism and resonance Raman spectroscopy (*6*, *24*, *77*). At this stage of the analysis, large differences are observed in the methyl shift pattern of the micellar low-spin cyano-cyt *c* compared with the same adduct without micelles. This provides evidence for a different electronic structure of the heme. Considering the structural aspects of the micellar cyt *c*, the NMR spectrum suggests a more open structure of the protein due to the scarcity of strongly paramagnetic shifted resonances (except heme protons) and the overlapping of the amide protons around 8 ppm. The same conclusions also apply for the data obtained with the studied diamagnetic species. Further research should give new insight for a more complete description of the structural changes induced by the micelles.

Electron self-exchange reaction between the micellar ferri- and ferro-cyt *c* has been used here to assign the heme methyl protons. We also estimate the rate constant and compared it with the value obtained using a redox mixture of micelle-free cyt *c*. Despite large differences between the two systems, the rates are similar. This is quite surprising considering, for example, the large previously reported variations from 2.8×10^4 to 2×10^7 at a ionic strength of 0.5 M for cyt *c* and cyt c_{551}, respectively (*66*). Because of the association with the micelles, we expect to find a compensation as well as complete reorganization of the charges on the surface of cyt *c*. This is likely to play a major role in controlling the electron self-exchange rate constant (*78*) and will require further work to be analyzed.

In summary, we demonstrate that NMR spectroscopy can be a judicious tool for investigating the structural changes of cyt *c* induced by micelles. Titration of the ferric native form with SDS micelles allows us to assess the importance of the protein/micelles ratio in controlling the extent of structural changes. In this way, intermediate species in moderately fast exchange can be related to the bis-histidine ligation. Further increase of the protein/micelles ratio causes the formation of a pentacoordinated high-spin species. Using this free binding site, we studied several derivatives in both the reduced and the oxidized states of the hemeprotein. The different forms of the heme methyl protons are assigned by means of exchange spectroscopy. The heme methyl shift pattern is different from the micelle-free cyt *c*, thus indicating a major variation of the heme electronic structure. The electron self-exchange of micellar cyano cyt *c* is estimated to be close to the value for the native protein. Further work is in progress that should lead to a better knowledge of protein−micelle interactions.

REFERENCES

1. McDonald, C. C., Phillips, W. D., and Vinogradov, S. N. (1969) *Biochem. Biophys. Res. Commun. 36*, 442−449.
2. Wüthrich, K. (1969) *Proc. Nat. Acad. Sci. U.S.A. 63*, 1071−1078.
3. Wüthrich, K. (1970) *Struct. Bonding (Berlin) 8*, 53−121.
4. Gadsby, P. M. A., Peterson, J., Foote, N., Greenwood, C., and Thomson, A. J. (1987) *Biochem. J. 246*, 43−54.
5. Barker, P. D., and Mauk, A. G. (1992) *J. Am. Chem. Soc. 114*, 3619−3624.
6. Oellerich, S., Wackerbarth, H., and Hildebrandt, P. (2002) *J. Phys. Chem. B 106*, 6566−6580.
7. Williams, G., Moore, G. R., Porteous, R., Robinson, M. N., Soffe, N., and Williams, R. J. P. (1985) *J. Mol. Biol. 183*, 409−428.
8. Williams, G., Moore, G. R., Porteous, R., Robinson, M. N., Soffe, N., and Williams, R. J. P. (1985) *J. Mol. Biol. 183*, 429−446.
9. Santos, H., and Turner, D. L. (1987) *FEBS Lett. 226*, 179−185.
10. Feng, Y., Roder, H., Englander, S. W., Wand, A. J., and Di Stefano, D. L. (1989) *Biochemistry 28*, 195−203.
11. Feng, Y., Roder, H., and Englander, S. W. (1990) *Biophys. J. 57*, 15−22.
12. Banci, L., Bertini, I., Gray, H. B., Luchinat, C., Reddig, T., Rosato, A., and Turano, P. (1997) *Biochemistry 36*, 9867−9877.
13. Banci, L., Bertini, I., Huber, J. G., Spyroulias, G. A., and Turano, P. (1999) *J. Biol. Inorg. Chem. 4*, 21−31.
14. Keilin, D., and Hartree, E. F. (1940) *Nature 145*, 934.
15. Shipley, G. G., Leslie, R. B., and Chapman, D. (1969) *Nature 222*, 561−562.

16. Gulik-Krzywicki, T., Shechter, E., Luzzati, V., and Faure, M. (1969) *Nature 223*, 1116−1121.
17. Nicholls, P. (1974) *Biochim. Biophys. Acta 346*, 261−310.
18. Burkhard, R. K., and Stolzenberg, G. E. (1972) *Biochemistry 11*, 1672−1677.
19. Takeda, K., Takahashi, K., and Batra, P. P. (1985) *Arch. Biochem. Biophys. 236*, 411−417.
20. Hiramatsu, K., and Yang, J. T. (1983) *Biochim. Biophys. Acta 743*, 106−114.
21. Yoshimura, T. (1988) *Arch. Biochem. Biophys. 264*, 450−461.
22. Muga, A., Mantsch, H. H., and Surewicz, W. K. (1991) *Biochemistry 30*, 7219−7224.
23. Gebicka, L., and Gebicki, J. L. (1999) *J. Protein Chem. 18*, 165−172.
24. Das, T. K., Mazumdar, S., and Mitra, S. (1998) *Eur. J. Biochem. 254*, 662−670.
25. Cortese, J. D., Voglino, A. L., and Hackenbrock, C. R. (1995) *Biochim. Biophys. Acta 1228*, 216−228.
26. Cortese, J. D., Voglino, A. L., and Hackenbrock, C. R. (1998) *Biochemistry 37*, 6402−6409.
27. Jemmerson, R., Liu, J., Hausauer, D., Lam, K. P., Mondino, A., and Nelson, R. D. (1999) *Biochemistry 38*, 3599−3609.
28. Pinheiro, T. J. T. (1994) *Biochimie 76*, 489−500.
29. Spooner, P. J. R., and Watts, A. (1991) *Biochemistry 30*, 3871−3879.
30. Pinheiro, T. J. T., Cheng, H., Seeholzer, S. H., and Roder, H. (2000) *J. Mol. Biol. 303*, 617−626.
31. Bertini, I., Turano, P., and Vila, A. J. (1993) *Chem. Rev. 93*, 2833−2932.
32. La Mar, G. N., and de Ropp, J. S. (1993) in *NMR of Paramagnetic Molecules* pp 1−78, Plenum Press, New York.
33. NMR and EPR (2000) *The Porphyrin Handbook* (Kadish, K. M., Smith, K. M. and Guilard, R., Eds.) Vol. 5, Academic Press, San Diego.
34. Bondon, A., and Mouro, C. (1998) *J. Magn. Reson. 134*, 154−157.
35. Mouro, C., Bondon, A., Jung, C., Hoa, G. H. B., De Certaines, J. D., Spencer, R. G. S., and Simonneaux, G. (1999) *FEBS Lett. 455*, 302−306.
36. Mouro, C., Bondon, A., Jung, C., De Certaines, J. D., and Simonneaux, G. (2000) *Eur. J. Biochem. 267*, 216−221.
37. Gupta, R. K., and Redfield, A. G. (1970) *Science 169*, 1204−1206.
38. Hong, X. L., and Dixon, D. W. (1989) *FEBS Lett. 246*, 105−108.
39. Rosell, F. I., Ferrer, J. C., and Mauk, A. G. (1998) *J. Am. Chem. Soc. 120*, 11234−11245.
40. Muthukrishnan, K., and Nall, B. T. (1991) *Biochemistry 30*, 4706−4710.
41. Colon, W., Wakem, L. P., Sherman, F., and Roder, H. (1997) *Biochemistry 36*, 12535−12541.
42. Yeh, S. R., and Rousseau, D. L. (1999) *J. Biol. Chem. 274*, 17853−17859.
43. Rajarathnam, K., La Mar, G. N., Chiu, M. L., Sligar, S. G., Singh, J. P., and Smith, K. M. (1991) *J. Am. Chem. Soc. 113*, 7886−7892.
44. La Mar, G. N., Jackson, J. T., Dugad, L. B., Cusanovich, M. A., and Bartsch, R. G. (1990) *J. Biol. Chem. 265*, 16173−16180.
45. La Mar, G. N., Budd, D. L., and Goff, H. (1977) *Biochem. Biophys. Res. Commun. 77*, 104−110.
46. La Mar, G. N., Davis, N. L., Johnson, R. D., Smith, W. S., Hauksson, J. B., Budd, D. L., Dalichow, F., Langry, K. C., Morris, I. K., and Smith, K. M. (1993) *J. Am. Chem. Soc. 115*, 3869−3876.
47. Bertini, I., Dikiy, A., Luchinat, C., Macinai, R., and Viezzoli, M. S. (1998) *Inorg. Chem. 37*, 4814−4821.
48. de Jongh, H. H., Ritsema, T., and Killian, J. A. (1995) *FEBS Lett. 360*, 255−260.
49. Schejter, A., Plotkin, B., and Vig, I. (1991) *FEBS Lett. 280*, 199−201.
50. Bren, K. L., Gray, H. B., Banci, L., Bertini, I., and Turano, P. (1995) *J. Am. Chem. Soc. 117*, 8067−8073.
51. Viola, F., Aime, S., Coletta, M., Desideri, A., Fasano, M., Paoletti, S., Tarricone, C., and Ascenzi, P. (1996) *J. Inorg. Biochem. 62*, 213−222.
52. Yao, Y., Qian, C., Ye, K., Wang, J., Bai, Z., and Tang, W. (2002) *J. Biol. Inorg. Chem. 7*, 539−547.
53. Yao, Y., Wu, Y., Qian, C., Ye, K., Wang, J., and Tang, W. (2003) *Biophys. Chem. 103*, 13−23.
54. Legrand, N., Bondon, A., and Simonneaux, G. (1996) *Inorg. Chem. 35*, 1627−1631.
55. Schejter, A., and Aviram, I. (1970) *J. Biol. Chem. 245*, 1552−1557.
56. Mathews, A. J., and Brittain, T. (1991) *Biochem. J. 276*, 121−124.
57. Theorell, H., and Akesson, A. (1941) *J. Am. Chem. Soc. 63*, 1812−1818.
58. Smith, M., and McLendon, G. L. (1981) *J. Am. Chem. Soc. 103*, 4912−4921.
59. Yamamoto, Y. (1996) *J. Biochem. 119*, 16−22.
60. Brennan, L., and Turner, D. L. (1997) *Biochim. Biophys. Acta 1342*, 1−12.
61. Burns, P., and La Mar, G. N. (1979) *J. Am. Chem. Soc. 101*, 5844−5846.
62. Burns, P., and La Mar, G. (1981) *J. Biol. Chem. 256*, 4934−4939.
63. Taler, G., Becker, O. M., Navon, G., Qin, W., Margoliash, E., and Schejter, A. (1999) *Biophys. Chem. 79*, 193−197.
64. Schejter, A., and Plotkin, B. (1988) *Biochem. J. 255*, 353−356.
65. Bellelli, A., Antonini, G., Brunori, M., Springer, B. A., and Sligar, S. G. (1990) *J. Biol. Chem. 265*, 18898−18901.
66. Dixon, D., Hong, X., and Woehler, S. (1989) *Biophys. J. 56*, 339−351.
67. Elöve, G. A., Bhuyan, A. K., and Roder, H. (1994) *Biochemistry 33*, 6925−6935.
68. Yeh, S. R., Takahashi, S., Fan, B., and Rousseau, D. L. (1997) *Nat. Struct. Biol. 4*, 51−56.
69. Telford, J. R., Tezcan, F. A., Gray, H. B., and Winkler, J. R. (1999) *Biochemistry 38*, 1944−1949.
70. Hildebrandt, P., and Stockburger, M. (1989) *Biochemistry 28*, 6710−6721.
71. Hildebrandt, P., Heimburg, T., and Marsh, D. (1990) *Eur. Biophys. J. 18*, 193−201.
72. Banci, L., Bertini, I., Bren, K. L., Gray, H. B., Sompornpisut, P., and Turano, P. (1995) *Biochemistry 34*, 11385−11398.
73. Banci, L., Bertini, I., Liu, G., Lu, J., Reddig, T., Tang, W., Wu, Y., Yao, Y., and Zhu, D. (2001) *J. Biol. Inorg. Chem. 6*, 628−637.
74. Liu, G., Chen, Y., and Tang, W. (1997) *J. Chem. Soc., Dalton Trans.* 795−801.
75. Yeh, S. R., and Rousseau, D. L. (1998) *Nat. Struct. Biol. 5*, 222−228.
76. Hagen, S. J., Latypov, R. F., Dolgikh, D. A., and Roder, H. (2002) *Biochemistry 41*, 1372−1380.
77. Pinheiro, T. J. T., Elöve, G. A., Watts, A., and Roder, H. (1997) *Biochemistry 36*, 13122−13132.
78. Koppenol, W. H., and Margoliash, E. (1982) *J. Biol. Chem. 257*, 4426−4437.
79. Santos, H., and Turner, D. L. (1986) *FEBS Lett. 194*, 73−77.

BI035044+